



Dedicated to the memory of
Professor Eugen Segal (1933-2013)

SYNTHESIS AND CHARACTERIZATION OF GLASS-CERAMIC SUPERCONDUCTORS IN (Pb, B)-DOPED Bi-Sr-Ca-Cu-O SYSTEM

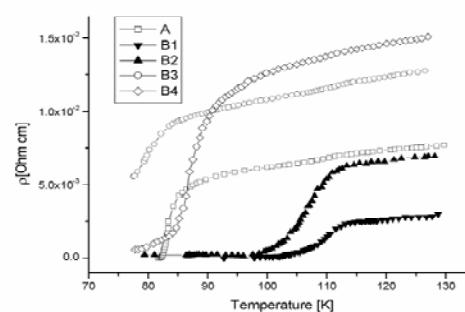
Victor FRUTH,^{a,*} Georgeta TANASE,^a Irina ATKINSON,^a Jeanina PANDELE CUSU,^a
Gheorghe ALDICA^b and Maria ZAHARESCU^a

^a Ilie Murgulescu Institute of Physical Chemistry of the Roumanian Academy,
202 Splaiul Independentei, 060021 Bucharest Roumania

^b National Institute for Research and Development in Materials Physics,
105bis Atomistilor, 077125-Magurele, Roumania

Received April 30, 2014

Glass-ceramic superconductors in the Bi-Sr-Ca-Cu-O system were prepared by melt-quenching method in the presence of some additives (Pb, B). The studied glasses were characterized by scanning electron microscopy (SEM), X-ray diffraction (XRD), thermogravimetric and differential thermal analysis (DTA/TGA) and differential scanning calorimetry (DSC). On the crystallized ceramics obtained by the annealing the glasses, transport resistance and XRD measurements were also done. The glass transition temperatures (T_g) was found to range in the 380-430 °C domain, followed by a set of exothermal effects that could be assigned to the crystallization of the superconducting phases. The nucleation and growth of the crystals is influenced by both the nature of the oxides used as additives and by their ratio. So, the samples doped with low amount of B ($x=0.1$ and 0.2) present obvious transitions at about 110 K, highlighting the presence of the 2223 phase in highest amount and well interconnected.



INTRODUCTION

Since high-temperature superconductors were discovered by Maeda *et al.* in 1988¹ in the Bi-Sr-Ca-Cu-O system, intensive studies were made on finding ways to enhance the growth of $\text{Bi}_2\text{Sr}_2\text{Ca}_2\text{Cu}_3\text{O}_x$ (2223) high T_c phase in order to increase its volume fraction in the prepared samples.²⁻⁴ The interest for obtaining the $\text{Bi}_2\text{Sr}_2\text{Ca}_2\text{Cu}_3\text{O}_x$ (2223) phase was determined by its highest superconducting transition ($T_c \approx 108$ K) as compared to the transitions presented by the

$\text{Bi}_2\text{Sr}_2\text{Ca}_1\text{Cu}_2\text{O}_y$ (2212) ($T_c \approx 95$ K) and $\text{Bi}_2\text{Sr}_2\text{Cu}_1\text{O}_z$ (2201) ($T_c \approx 20$ K) phases. Partial substitution of Bi for Pb in the Bi-Sr-Ca-Cu-O system has been found to sharply increase the volume fraction of the (2223) high- T_c phase.⁵ The first method used for preparing bismuth based superconductors (BSCCO) was the conventional ceramic route,^{1, 6-8} but other alternative preparation methods were also established. Wet methods of preparation as oxalic coprecipitation was developed by Takano *et al.*,⁵ Huang *et al.*,⁹ or Popa *et al.*¹⁰⁻¹⁵ Sol-gel method was also reported in many papers¹⁶⁻²²

* Corresponding author: vfruth@gmail.com

and micro-emulsion-base techniques were also applied.

Komatsu *et al.*²³ used the so-called glass ceramics route to prepare ceramic materials of this category. Using X-ray diffraction and DTA analysis, the authors observed that some samples, obtained by melt quenching with the $\text{Bi}_{1.5}\text{SrCaCu}_2\text{O}_x$ and $\text{Bi}_{0.5}\text{Pb}_{0.5}\text{SrCaCuO}_x$ compositions were amorphous (vitreous). Following thermal treatments over 800°C the materials become superconductors. That is why Komatsu proposed that the superconductors obtained by recrystallization of vitreous phases should be called "high- T_c superconducting glass ceramics". Simultaneously, Hinks *et al.*²⁴ and Tsutomu *et al.*²⁵ extended this preparation technique to other Bi based superconductors.

More recently, Gazda *et al.*²⁶ studied the electronic conduction in Bi-based materials with superconducting properties while Nilson *et al.*²⁷ realized a comprehensive study of the critical aspects on the preparation of 2223 glassy precursors by melt-process.

Obtaining superconductors by using glass-ceramic route is an attractive method offering some advantages such as:²⁸⁻³² high homogeneity, the possibility to control the crystal growth, preferential orientation of superconductive phases, controlled development of defects (nanometric phases smaller than the coherence length of the superconducting phase so that it can constitute a pinning center), obtaining of fibers, thick films and ceramic bodies with various shapes, etc. The method presents also some disadvantages, among which the most important are: compositional variation during the melting process or the variation of cations' oxidation state.

The aim of this work is to obtain homogeneous and stable glasses in the Bi-Sr-Ca-Cu system in the presence of some additives (Pb, B) and to study their crystallization in order to establish the conditions of the formation of the high T_c 2223 phase. Besides PbO co-doping with B_2O_3 has been chosen due to its recognized glass forming ability and very low melting temperature.

EXPERIMENTAL

1. Samples preparation

The investigated samples had the nominal compositions that can be described by the general formula $\text{Bi}_{1.6}\text{Pb}_{0.4-x}\text{B}_x\text{Sr}_2\text{Ca}_2\text{Cu}_3\text{O}_y$ (where $x=0, 0.1, 0.2, 0.3$ and 0.4 , representing the B_2O_3 substitution of PbO). This formula was chosen in

order to respect the stoichiometry of high T_c phase in Bi-Sr-Ca-Cu-O system and to investigate the effects produced by the nature and content of the additive oxides. These substitute oxides must help to obtain glasses with homogeneous composition and with highest stability. It has to be mentioned that both substitute oxides (PbO and B_2O_3) have low melting point: $t = 888$ °C for PbO and 450 °C for B_2O_3 , respectively. Additionally, B_2O_3 has been chosen due to its recognized glass forming ability.

Corresponding amounts of Bi_2O_3 , SrCO_3 , CaCO_3 , CuO, PbO and B_2O_3 were adjusted to obtain the nominal desired composition. The powders were mixed for 1h in an agate mortar to get a homogeneous mixture. This mixture was melted in air for 10 min at 1200 °C. The melted samples were then rapidly quenched between two cooper plates.

Shiny black amorphous glasses sheets were obtained. Part of the glass sheets were then crushed and ground in an agate mortar and die pressed and annealed at different temperatures. The undoped samples were labelled A, and the doped samples were labelled B1- B4, according to the Boron content.

2. Samples characterization

The crystallization of the glasses was investigated by DTA/TG analysis using Mettler Toledo 851° equipment and a DSC Mettler Toledo 823° apparatus, from room temperature up to 1000 °C in the case of DTA/TG measurements and 700 °C for DSC investigations, with heating rate of 2, 5 and 10 °C/min.

The surface morphology of the samples (glasses and ceramics) was investigated by SEM-EDS technique with a JEOL 5600 microscope.

The formation of crystalline phases was examined by the XRD method using Shimatzu XRD 6000 equipment with monochromatic CuK_α radiation. The ICDD files have been used for phase identification.

We used the standard DC four-probe technique to measure resistance temperature (R-T) plot in zero magnetic fields. The soldering/sticking method enabled to obtain low contact specific strengths, of about 10^{-4} Ωcm^2 at 77 K, which also presents a considerable mechanical strength. The dependence of the magnetic susceptibility on the temperature was measured using a Hartschon bridge, in alternative current, at 40 A/m and 285 Hz, beginning with the environment temperature of 77 K.

RESULTS

In the experimental conditions used shiny black amorphous glasses were obtained. The vitreous state was confirmed by the diffraction patterns specific to glasses (not presented here).

SEM observations in cross section have shown a homogeneous vitreous phase. The same method on spots showed that the obtained glasses present slight surface crystallization (Fig. 1) due to the fact that at surface the kinetic process is different from the bulk. The surface crystallization is hindered in the samples with increasing B content, confirming its recognized glass forming ability.

The thermal behavior of the resulted samples was established by DTA/TGA measurements. In Fig. 2 the characteristic curves are presented for the B1 sample that contains the lowest amount of B_2O_3 . A DSC curve for the same sample is also presented in Fig. 3, where the thermal effects are better underlined.

DTA measurements on glasses show that glass transition (T_g) occur in the 380–430 °C temperature range, decreasing with the increasing of the B_2O_3 content. Simultaneously with the glass transition, in the TG curve, a small but continuous weight increasing is observed up to 700 °C that could be assigned to the oxidation of the Cu_2O contained in the obtained glasses. The presence of Cu_2O in the Bi-Sr-Ca-Cu-O based glasses is expected and was also previously observed and discussed.³³

On may notice that the glass transition is followed by a set of exothermal effects that could be assigned to the crystallization of the

superconducting phases. Two better defined peaks at approximately 450 and 470 °C are consistently present, while the next exothermal events were smaller and broader.

The first exothermal effect is assigned to the crystallization of the 2201 phase no matter of the presence and nature of dopants. It has to be underlined that, in the doped samples the formation of crystals of 2212 phase, at low temperatures (about 500 °C) was also noticed. This observation could be connected to a new mechanism of superconductive phases formation, suggesting the simultaneous appearance of 2201 and 2212 phases. This effect is facilitated by the change of thermodynamic conditions, induced by dopants presence. At 800 °C the 2201 phase disappears and an accelerated crystallization process of the 2212 phase was observed. The high T_c phase (2223) is obtained only after prolonged thermal treatments in a narrow range of temperatures (825–855 °C).

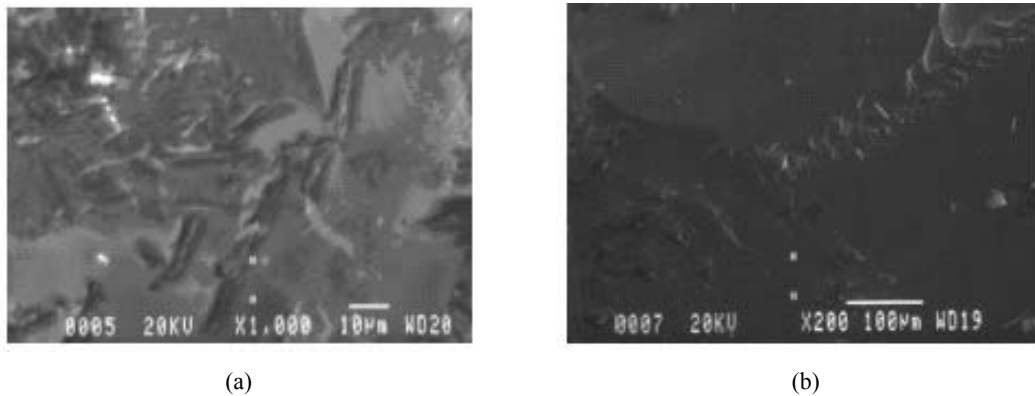


Fig. 1 – SEM images of the surface of the obtained glasses with B1 (a) and B4 (b) composition.

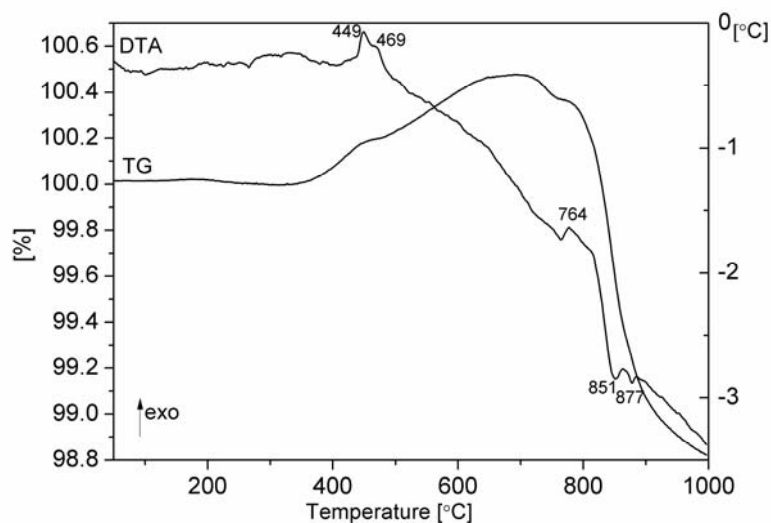


Fig. 2 – DTA/TG curves of the glass of composition B1 ($Bi_{1.6}Pb_{0.4-x}B_{0.1}Sr_2Ca_2Cu_3O_y$); heating rate 10°C/min.

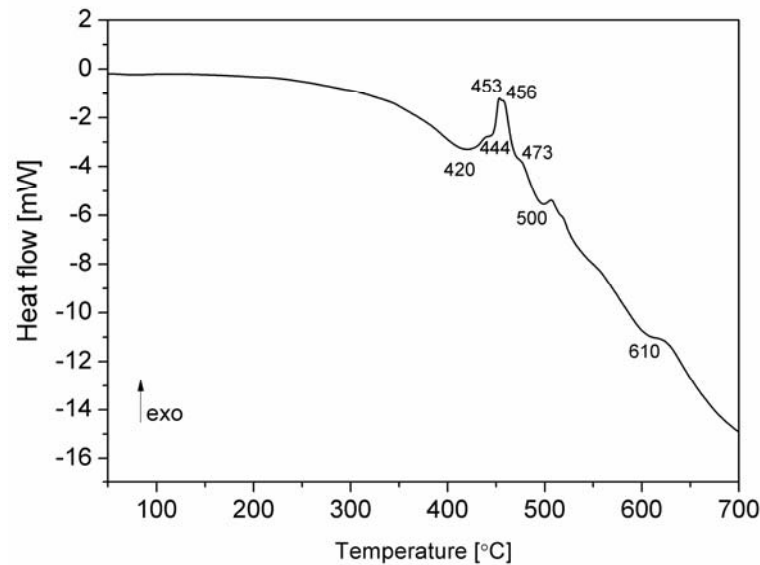


Fig. 3 – DSC curve of the B1 glass; heating rate 10 °C/min.

Table 1

List of thermal effects of glass samples as determined by DSC measurements

Sample	Thermal effects	
	T _g (°C)	T _{ex(exo)} (°C)
A	430	450; 470*; 510; 640
B1	420	444; 456*; 473; 500; 610
B2	423	440*; 452; 595; 665
B3	420	430*; 445; 595; 645
B4	382	433; 460*; 525; 665

* main effect

An attempt to calculate the activation energy of glass crystallization process in nonisothermal conditions was done only for the first crystallization effects that occur in the 400-500 °C temperature range and they are assigned to formation of the 2201 and 2212 phases.

The nonisothermal kinetic equation of Kissinger was used.³⁴ The basic relation was modified by Matusita and Sakka³⁵ and is known as an extension of the Johnson-Mehl-Aavrami kinetic model.^{36, 37} The results obtained with the Kissinger equation were compared with those obtained using the Ozawa equation.³⁸

The Kissinger equation is expressed as:

$$\ln(\beta/T_{\max}^2) = E_a/RT_{\max} + c \quad (1)$$

and Ozawa equation is expressed as:

$$\log(\beta) = -0.4567 E_a/RT + c \quad (2)$$

where β is the heating rate, R is the gas constant, T_{\max} is the crystallization peak temperature, E_a is the activation energy for the crystal growth, and c is a constant. The plots of $\ln(\beta/T_{\max}^2)$ and $\log(\beta)$

versus $1000/T$ with heating rates of 2, 5 and 10 K/min were used to find the activation energy of the process of crystallization. The corresponding curves for the sample B1 with the lowest Boron content are presented in the Figs. 4 and 5 and the activation energy obtained by both methods are summarized in Table 2.

The determined values of the activation energy for the crystallization of the 2201 phase in B1 sample are in the same range of magnitude with those reported in previous studies³⁹⁻⁴¹ for BSCCO glass crystallizations (70- 430 kJ/mol). The second effect is assigned to subsequent crystallization of low amount of 2212 phase.

For the other samples, with higher amount of Boron, the activation energy of the crystallization process was established to be in the range of 250-340 kJ/mol, decreasing with the B_2O_3 content.

Comparing our results with values presented by previous studies it can be noticed that the addition of B_2O_3 decreased the crystallization activation energy of the Pb, B co-doped BSCCO system.

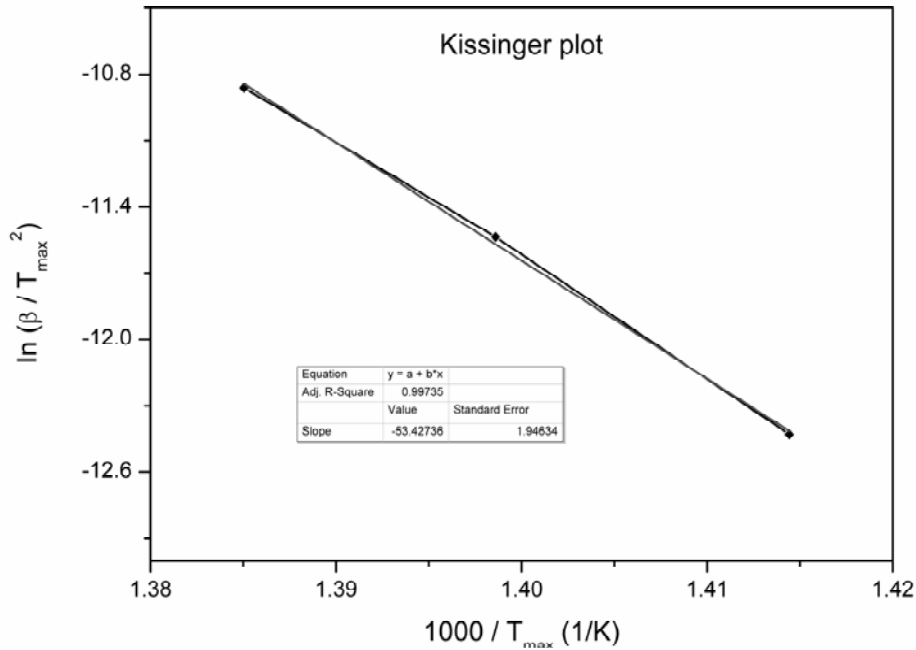


Fig. 4 – Plots of $\ln(\beta/T_{\max}^2)$ (Kissinger equation) versus $1000/T$ with heating rates of 2, 5 and 10 K/min for the sample B1 ($\text{Bi}_{1.6}\text{Pb}_{0.3}\text{B}_{0.1}\text{Sr}_2\text{Ca}_2\text{Cu}_3\text{O}_y$).

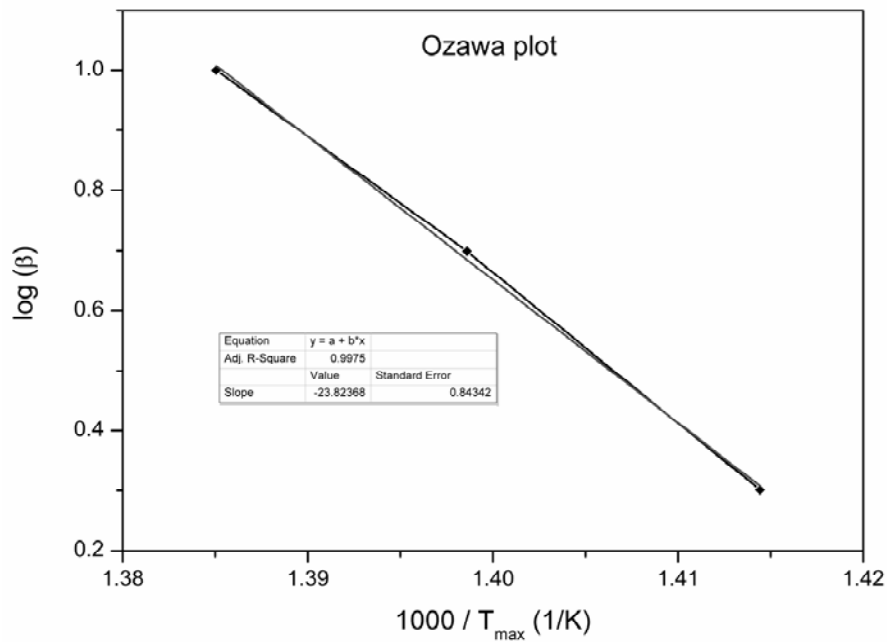


Fig. 5 – Plots of $\log(\beta)$ versus $1000/T$ (Ozawa equation) with heating rates of 2, 5 and 10 K/min for the B1 ($\text{Bi}_{1.6}\text{Pb}_{0.3}\text{B}_{0.1}\text{Sr}_2\text{Ca}_2\text{Cu}_3\text{O}_y$) sample.

Table 2

Activation Energies, E , for Initial Crystal Growth of Bulk Bi-Based Glasses Evaluated by Nonisothermal DTA Experiments

$\text{Bi}_{1.6}\text{Pb}_{0.3}\text{B}_{0.1}\text{Sr}_2\text{Ca}_2\text{Cu}_3\text{O}_y$ (sample B1)		1 st exo effect			2 nd exo effect		
		2	5	10	2	5	10
Heating rate (K/min)							
T_{\max} (K)		707	715	722	731	740	744
Activation energy (kJ/mol)	Kissinger eq.	444.195			503.930		
	Ozawa eq.	433.698			490.860		

The crystallization behavior of the samples was confirmed by XRD. At 800 °C, 2201 phase disappears and an accelerated crystallization process of 2212 phase was observed (Figs. 6 and 7). The high T_c phase (2223) is obtained only after prolonged thermal treatments in a narrow range of temperatures (825÷855°C). The most intense diffraction lines were taken into consideration for evaluating the crystallization of the superconducting phases depending on the composition and thermal treatment temperatures. For the 2212 phase the following diffraction lines were taken into consideration: (2,0,0) line with 100% intensity, (1,1,5) line with 92% intensity,

(1,1,7) line with 75% intensity and (1,1,3) line with 29% intensity (ICDD file. 00-046-0780).

The crystallization processes were examined from the point of view of the applied thermal treatments as well as of the investigated composition. This continuous applied thermal treatment put in evidence the nucleation and crystal growth processes correlated with the presence of the substituted oxides. The lead presence promoted the formation of numerous nucleation centers and small and uniform crystals while the presence of boron induced much higher superconducting crystals formation but reduced their number.

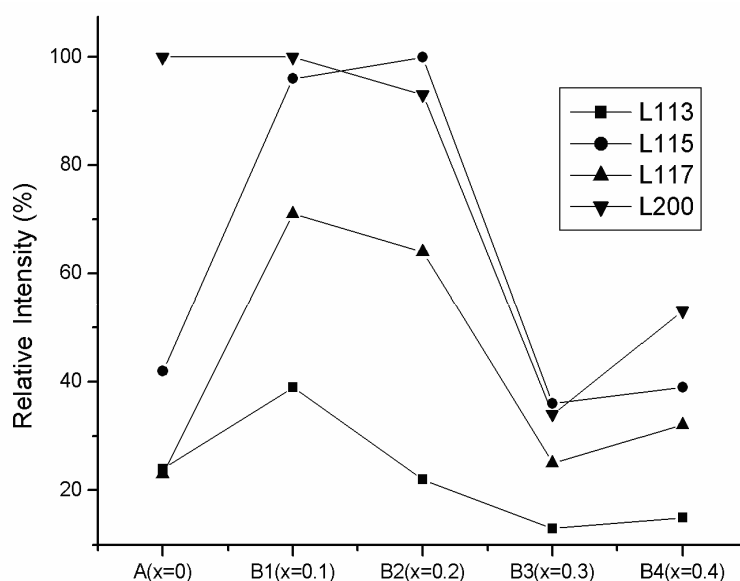


Fig. 6 – Relative intensities of the characteristic diffraction lines L (h,k,l) of the 2212 phase for the B1 ($\text{Bi}_{1.6}\text{Pb}_{0.3}\text{B}_{0.1}\text{Sr}_2\text{Ca}_2\text{Cu}_3\text{O}_y$) sample, annealed 825 °C/20h.

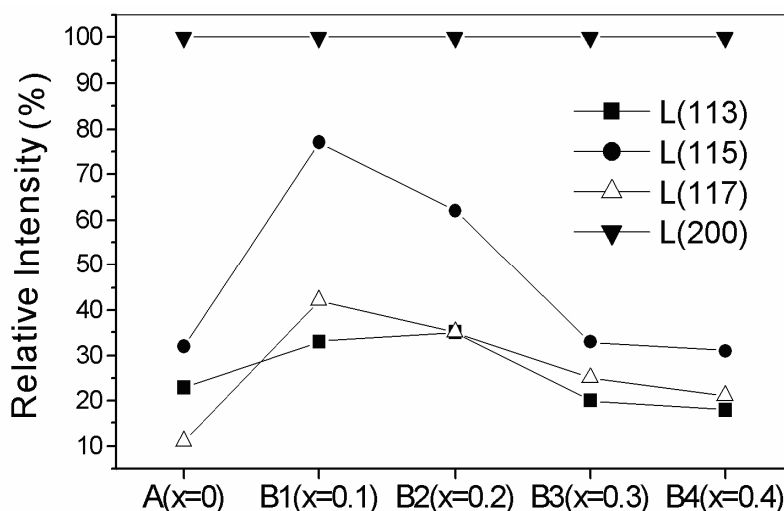


Fig. 7 – Relative intensities of the characteristic diffraction lines L (h,k,l) of the 2212 phase for the B1 ($\text{Bi}_{1.6}\text{Pb}_{0.3}\text{B}_{0.1}\text{Sr}_2\text{Ca}_2\text{Cu}_3\text{O}_y$) sample, annealed 830 °C/48h.

The morphology and the texture of the samples are decisive for their physical characteristics. Fig. 6. The density of the ceramic samples is smaller than that of the vitreous precursors. This observation can be explained by the texture conferred by the crystallized phases (bidimensional and generally randomly orientated), as well as by the nature and ratio of the additional used oxides. It can also be mentioned important variations compared to the

precursor glasses when the content in boron increases. The temperature and time of crystallization plays also an important role on the samples morphology as shown in Figs. 8 and 9.

The variation of the electric resistivity with temperature and the dependence of the magnetic susceptibility on temperature were also determined. The results of the undertaken measurements are given in Table 3.

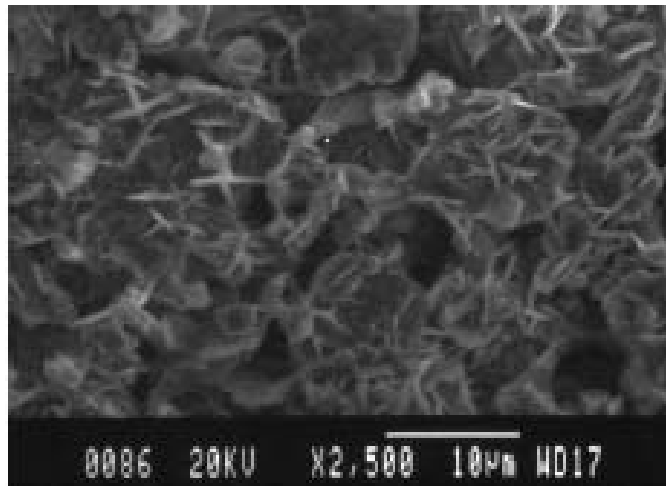


Fig. 8 – SEM image of the ceramics after annealing at 825 °C/20h for B1 ($\text{Bi}_{1.6}\text{Pb}_{0.3}\text{B}_{0.1}\text{Sr}_2\text{Ca}_2\text{Cu}_3\text{O}_y$) sample.

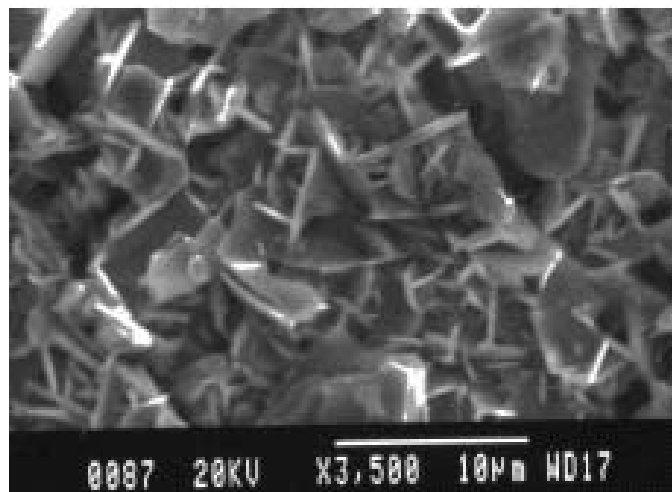


Fig. 9 – SEM image of the ceramics after annealing at 830 °C /48h for B1 ($\text{Bi}_{1.6}\text{Pb}_{0.3}\text{B}_{0.1}\text{Sr}_2\text{Ca}_2\text{Cu}_3\text{O}_y$) sample.

Table 3

Superconducting transition parameters in the samples described by the formula $\text{Bi}_{1.6}\text{Pb}_{0.4-x}\text{B}_x\text{Sr}_2\text{Ca}_2\text{Cu}_3\text{O}_y$

Sample	Annealing treatment °C/20 h	Parameters					
		T_c (onset) K	T_c (midpoint) K	T_c (R=0)	ΔT_{c1} (10%-90%)	$\rho_{300K}/\rho_{\text{onset}}$	$J_c(77K;0T)$ A/cm ²
A	830	114	83.5	81.7	25	1.75	-
B1	830	115	109.5	98	9	2.7	36
B2	830	117	107.5	93	10	1.75	30
B3	830	113	~77	< 77	-	1.7	-
B4	830	97	87.5	< 77	11	-	-

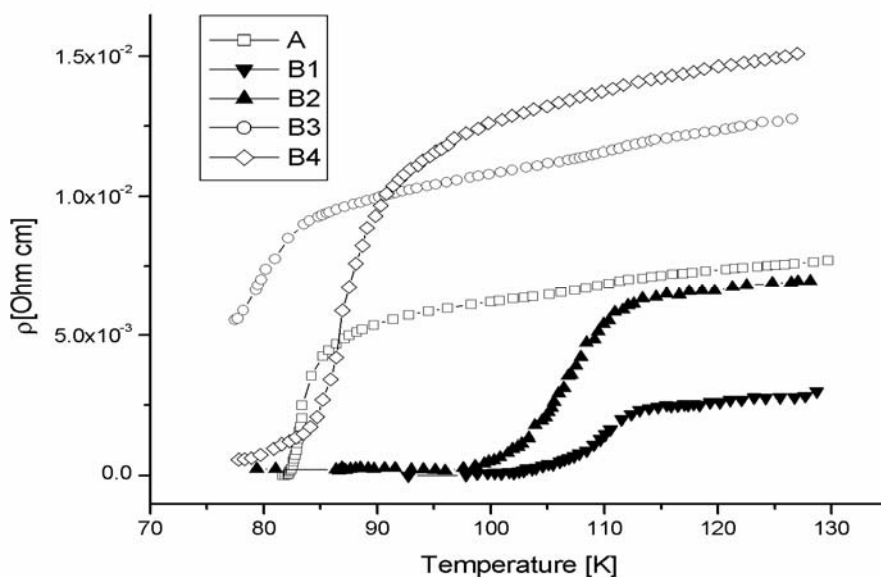


Fig. 10 – The variation of the electric resistance with temperature for the annealed samples at 830 °C/48h.

Fig. 10 presents the resistivity variation curves normalized with temperature for the investigated samples, prepared in the same conditions, but with a different content of Pb and B. All samples show a behavior of the metallic conduction which has an almost linear dependency and a ratio $\rho_{300K}/\rho_{onset} = 1.6 \div 2.7$. Samples A, B3 and B4 show a small resistivity decrease at 114, 113 K, and respectively 93 K, determined by the 2223 phase presence in the samples, according to diffraction measurements of the corresponding glass-ceramics. But B1 and B2 samples present obvious transitions at about 110 K, highlighting the 2223 phase proportion which is significantly higher and well interconnected/linked.

The superconducting transition of the B1 and B2 samples takes place at 98 K, respectively 93 K due to the existence of resistive foot determined by the presence of some trace phases in the samples. In order to determine the weight of the 2223 phase in the volume, the variation of the magnetic susceptibility (χ) with temperature was recorded for sample B1. The profile of the curve (χ) = f(T) (not presented here) shows that in the samples there two superconducting phases are present, with the T_c temperatures at 76 K and 104 K respectively, suggesting that the prevalent phase in the sample is 2212 phase. The volume fraction of the phase with the highest superconducting transition temperature which is (2223) is estimated to 10%.

The electric and magnetic behaviors are well correlated with the presence of the phases and the morphology of the samples obtained by glass

ceramic route. So, B1 and B2 samples present obvious transitions at about 110 K, highlighting the 2223 phase proportion which is significantly higher and well interconnected. Although the measured values of the critical current densities do not present a significant performance, they suggest that there are possibilities of improving the characteristics of the glass ceramics with B1 composition and noticed that the presence of B_2O_3 , in a proper proportion enhanced the quality of the precursor glasses and superconducting properties of the sintered glass ceramics.

CONCLUSIONS

In the present paper the possibility of obtaining glass ceramics with relevant superconducting properties of which composition is expressed by the formula $Bi_{1.6}Pb_{0.4-x}B_xSr_2Ca_2Cu_3O_y$ (where $x = 0.1; 0.2; 0.3; 0.4$) was established. The best results were obtained for the compositions in which B ratio was rather small ($x=0.1$ and 0.2).

The results obtained allowed to conclude that nucleation and growth of the crystals, in glass ceramic route, can be influenced by both the nature of the supplementary used oxide and by its ratio. In the samples without or in those with only PbO addition, the crystals are smaller and more numerous, involving the formation of a great number of crystallization germs in the vitreous matrix.

The presence of B_2O_3 enhanced the glass formation ability of the reaction mixture and facilitated the crystallization of the 2223 high T_c phase.

REFERENCES

1. H. Maeda, Y. Tanaka, M. Fukutumi and T. Asano, *Jpn. J. Appl. Phys.*, **1988**, 27, L209-L210.
2. E. Takayama-Muromachi, Y. Uchida, A. Ona, F. Izumi, M. Onoda, Y. Matsui, K. Kasuda, S. Takekawa and K. Kato, *Jpn. J. Appl. Phys.*, **1988**, 27, 365-368.
3. N. F. Mott, *J. Phys.: Condensed Matter*, **1993**, 5, 3487-4506.
4. P. W. Andersen, *Science*, **1987**, 235, 1196-1198.
5. M. Takano, J. Takada, K. Oda, H. Kitaguchi, Y. Miura, Y. Ikeda, Y. Tomii and H. Mazaki, *Jpn. J. Appl. Phys.*, **1988**, 27, L1041-L1043.
6. I. Teoreanu, V. Fruth, M. Zaharescu and G. Tănase, *Rev. Roum. Chim.*, **1995**, 40, 1003-1009.
7. I. Hamadneh, A. Agil, A.K. Yahya and S. A. Halim, *Physics C*, **2007**, 463-465, 207-210.
8. M. Zaharescu, V. Fruth, M. Popa, G. Tănase, N. Drăgan and I. Teoreanu, *J. Eur. Ceram. Soc.*, **1998**, 18, 1251-1255.
9. Y.T. Huang, D. S. Shy and L. J. Chen, *Physica C*, **1998**, 294, 140-146.
10. M. Popa, M. Zaharescu, L. Marta, L. Diamandescu and A. Toțovână, *Key Eng. Mater.*, **1997**, 132-136, 1254-1258.
11. M. Popa, A. Toțovână, L. Popescu, N. Drăgan and M. Zaharescu, *J. Eur. Ceram. Soc.*, **1998**, 18, 1265-1271.
12. M. Popa, J. M. Calderon-Moreno, D. Crișan and M. Zaharescu, *J. Thermal Anal. Cal.*, **2000**, 62, 633-645.
13. M. Popa and M. Zaharescu, *Rev. Roum. Chim.*, **2000**, 45, 907-913.
14. M. Popa, J. M. Calderon-Moreno, D. Crișan and M. Zaharescu, *J. Thermal Anal. Cal.*, **2000**, 62, 633-645.
15. M. Popa, J. Calderon-Moreno and M. Zaharescu, *J. Eur. Ceram. Soc.*, **2000**, 20, 2273-2278.
16. C. Y. Shieh, Y. Huang, M. K. Wu and C. Y. Hung, *Physica C*, **1991**, 185-189, 513-514.
17. S. A. Halim, S. Al- Khawaledh, H. Azhan, S. B. Mohoamed and K. Khalid, J. Suradi, *J. Mater. Sci.*, **2000**, 35, 3043-3046.
18. L. Marta, M. Zaharescu, L. Ciontea and T. Petrisor, *Applied Superconductivity*, **1993**, 1, 677-691.
19. L. Marta, L. Ciontea, T. Petrisor, M. Zaharescu, D. Crișan and Iv. Haiduc, *J. Sol-Gel Sci. Technol.*, 1994, 2, 437-441.
20. L. Marta, C. Sârbu, L. Zador, M. Zaharescu and D. Crișan, *J. Sol-Gel Sci. Technol.*, **1997**, 8, 681-684.
21. L. Marta and M. Zaharescu, *Rev. Roum. Chim.*, **2002**, 47, 1261-1266.
22. A. Tampieri, G. Celloti, S. Lesca, G. Bezzi, T.M.G. La Torretta and G. Magnani, *J. Eur. Ceram. Soc.*, **2000**, 20, 120-126.
23. T. Komatsu, R. Sato, K. Imai, K. Matusita and Y. Yamashita, *Jpn. J. Appl. Phys.*, **1988**, 27, L550-552.
24. D. G. Hinks, A. W. Mitchell, Y. Zheng, D. R. Richards and B. Dabrowski, *Appl. Phys. Lett.* **1989**, 54, 1585-1587.
25. M. Tsutomu, A. Yoshinori, T. Masahiro, T. Noboru and K. Yoshiyuki, *Jap. J. Appl. Phys. Part 2: Let.*, **1988**, 27, L777-L778.
26. M. Gazda, B. Kusz, S. Stizza, R. Natali, T. Klimczuk and L. Murawski, *J. Non-Cryst. Solids*, **2007**, 353, 1023-1029.
27. A. Nilsson, W. Gruner, J. Acker and K. Wetzig, *J. Non-Cryst. Solids*, **2008**, 354 839-847.
28. M. R. De Guire, N. P. Bansal and C. J. Kim, *J. Am. Ceram. Soc.*, **1990**, 73, 1165-1171.
29. N. P. Bansal, *J. Appl. Phys.*, **1990**, 68, 1143-1145.
30. T. G. Holesinger, D. J. Miller and L. S. Chumbley, *J. Mater. Res.*, **1992**, 7, 1658-1671.
31. V. Fruth, M. Zaharescu and G. Aldica, *Applied Superconductivity*, **1993**, 1, 693-707.
32. I. Teoreanu, V. Fruth, M. Zaharescu, G. Tănase and Zs. Hegedus, *Key Eng. Mater.*, **1997**, 132-136, 1235-1238.
33. T. Komatsu, R. Sato, Y. Kuken and K. Matusita, *J. Am. Ceram. Soc.*, **1993**, 76, 2795-2800.
34. H. E. Kissinger, *J. Res. Nat. Bur. Stand.*, **1956**, 57, 217-220.
35. K. Matusita and S. J. Sakka, *J. Non-Cryst. Solids*, **1980**, 38, 741-746.
36. M. J. Avrami, *Chem. Phys.* **1939**, 7, 1103-1106.
37. W. A. Johnson and R. F. Mehl, *Trans. Am. Inst. Elect. Eng.* **1939**, 135, 416-418.
38. T. Ozawa, *Bull. Chem. Soc. Jpn.*, **1965**, 38, 1881-1886.
39. T. Komatsu, R. Sato, H. Meguro, K. Matusita and T. Yamashita, *J. Mater. Sci.*, **1991**, 26, 683-688.
40. R. Sato, T. Komatsu, Y. Kuken and K. Matusita, *J. Non-Cryst. Solids*, **1993**, 152, 150-156.
41. T. S. Kayed, N. Calinli, E. Aksu, H. Koralay, A. Günen, İ. Ercan, S. Aktürk and Ş. Çavdar, *Cryst. Res. Technol.*, **2004**, 39, 1063-1069.

